STEM CELLS TRANSLATIONAL MEDICINE®

TISSUE ENGINEERING AND REGENERATIVE MEDICINE

Mesenchymal Stem Cell-Derived Extracellular Vesicles as Mediators of Anti-Inflammatory Effects: Endorsement of Macrophage Polarization

CLAUDIA LO SICCO,[a,b] DANIELE REVERBERI,[c] CAROLINA BALBI,[a] VALENTINA ULIVI,[a] ELISA PRINCIPI,[a] LUISA PASCUCCI,[d] PAMELA BECHERINI,[e,f] MARIA CARLA BOSCO,[e] LUIGI VARESIO,[e] CHIARA FRANZIN,[g] MICHELA POZZOBON,[g,h] RANIERI CANCEDDA,[a] ROBERTA TASSO[b]

Key Words. Extracellular vesicles • Mesenchymal stem cells • Inflammation • Macrophages • Cell hypoxia • Regenerative medicine

ABSTRACT

Mesenchymal Stem Cells (MSCs) are effective therapeutic agents enhancing the repair of injured tissues mostly through their paracrine activity. Increasing evidences show that besides the secretion of soluble molecules, the release of extracellular vesicles (EVs) represents an alternative mechanism adopted by MSCs. Since macrophages are essential contributors toward the resolution of inflammation, which has emerged as a finely orchestrated process, the aim of the present study was to carry out a detailed characterization of EVs released by human adipose derived-MSCs to investigate their involvement as modulators of MSC anti-inflammatory effects inducing macrophage polarization. The EV-isolation method was based on repeated ultracentrifugations of the medium conditioned by MSC exposed to normoxic or hypoxic conditions (EV^{Normo} and EV^{Hypo}). Both types of EVs were efficiently internalized by responding bone marrow-derived macrophages, eliciting their switch from a M1 to a M2 phenotype. In vivo, following cardiotoxin-induced skeletal muscle damage, EV^{Normo} and EV^{Hypo} interacted with macrophages recruited during the initial inflammatory response. In injured and EV-treated muscles, a downregulation of IL6 and the early marker of innate and classical activation Nos2 were concurrent to a significant upregulation of Arg1 and Ym1, late markers of alternative activation, as well as an increased percentage of infiltrating $CD206^{pos}$ cells. These effects, accompanied by an accelerated expression of the myogenic markers *Pax7*, *MyoD*, and *eMyhc*, were even greater following EV^{Hypo} administration. Collectively, these data indicate that MSC-EVs possess effective anti-inflammatory properties, making them potential therapeutic agents more handy and safe than MSCs. © STEM CELLS TRANSLATIONAL MEDICINE *2017;00:000–000*

SIGNIFICANCE STATEMENT

The rational control of inflammation, a universal response to injury, is a good candidate for triggering tissue repair. Mesenchymal stem cell (MSC) paracrine activity favors tissue repair modulating inflammation-associated immune cells. An alternative approach to regulate the inflammatory response is here proposed. This strategy relies on the use of extracellular vesicles (EVs) derived from human adipose tissue-derived MSCs as mediators of the anti-inflammatory effects, switching macrophages into an alternative activation profile. Despite the remaining challenges, these results highlight the importance of EVs as a handy cell-free approach guiding regenerative processes.

INTRODUCTION

Tissue repair, sometimes called healing, refers to the restoration of tissue architecture and function after an injury [1]. It is a multistep, dynamic process and consists of three consecutive and overlapping stages: inflammation, new tissue formation, and remodeling [2]. The transition from one stage to another is controlled and regulated by cell-released mediators, which are common to most regenerating tissues, with exception of some specialized ones, such as liver and skeletal tissues, that possess distinctive forms of regeneration and follow separate pathways [3]. There is an increasing evidence that the inflammatory microenvironment resulting from the initial cell interactions dictates how the healing process will proceed [4]. In particular, innate immune cells, such as macrophages, lead the inflammatory cascade reaction guiding revascularization and repair

[a]Department of Experimental Medicine, University of Genova, Genova, Italy; [b]U.O. Regenerative Medicine, IRCCS AOU San Martino-IST, National Cancer Research Institute, Genova, Italy; [c]U.O. Molecular Pathology, IRCCS AOU San Martino-IST, National Cancer Research Institute, Genova, Italy; [d]Department of Veterinary Medicine, University of Perugia, Perugia, Italy; [e]Molecular Biology Laboratory, Istituto Giannina Gaslini, Genova, Italy; [f]Department of Internal Medicine, University of Genova, Genova, Italy; [g]Stem Cells and Regenerative Medicine Lab, Fondazione Istituto di Ricerca Pediatrica Città della Speranza, Padova, Italy; [h]Department of Women and Children Health, University of Padova, Padova, Italy

Correspondence: Roberta Tasso, Ph.D., U.O. Regenerative Medicine, IRCCS AOU San Martino-IST, National Cancer Research Institute, Largo Rosanna Benzi 10, 16132, Genova, Italy. Telephone: 39-010-5558319; Fax: 39-010-555257; e-mail: robertatasso@gmail.com

Received August 4, 2016; accepted for publication November 29, 2016; published Online First on Month 00, 2017.

1066-5099/2017/$30.00/0

http://dx.doi.org/10.1002/sctm.16-0363

at injury sites [5, 6]. Diversity and plasticity are distinctive characteristics of macrophages. Classical M1 and alternative M2 activated macrophages represent two extremes of a dynamic state of activation. M1 macrophages exhibit potent antimicrobial properties, high capacity to present antigen, and consequent activation of Th1 responses. Conversely, M2 macrophages possess the capacity to facilitate tissue repair and regeneration [7].

The contribution of mesenchymal stem cells (MSCs) in tissue repair has been addressed in a variety of disease models [8, 9]. Contextually, their efficacy in the functional improvement of injured tissues was mostly related to a paracrine effect rather than a direct engraftment and differentiation [10–12]. We have recently demonstrated that in an inflammatory environment as the one generated during the early phases of the wound healing process, MSC paracrine activity was significantly modulated promoting a functional switch of macrophages from a pro- to an anti-inflammatory state, thus corroborating evidences showing that the mobilization of innate immune cells mediates the activation of regenerative processes [10, 13].

Among the factors responsible for the paracrine effects of MSCs, extracellular vesicles (EVs) have been recently described as new players in cell-to-cell communication by serving as vehicles for transfer between cells of membrane and cytosolic proteins, lipids, and genetic information [14, 15]. EVs are defined as a mixed population of membrane-surrounded structures with overlapping composition, density, and sizes, including exosomes, ectosomes, microvesicle particles, and apoptotic bodies in accordance with the recommendations of the International Society for Extracellular Vesicles (ISEV) [16].

Recent studies demonstrated that EVs represent physiologically relevant and powerful components of the MSC secretome, playing important roles in local induction of tissue regeneration [8, 12, 17]. In the present study, we focused on the detailed characterization of EVs released by human adipose tissue-MSCs to evaluate if the crosstalk between MSCs and cells of the innate immunity could be carried out by secreted EVs and if these interactions occur also in a regenerative microenvironment as the one generated following skeletal muscle damage. To mimic the typical environment established during tissue injury, EVs were isolated from the conditioned medium of MSCs harvested under both normoxic and hypoxic culture conditions (EV^{Normo} and EV^{Hypo}, respectively). We here report that both types of vesicles acted as mediators of the dynamic interplay between MSCs and cells of the innate immunity in vitro and in vivo. EVs effectively triggered the macrophage proliferation and polarization from a M1 to a M2 phenotype. Of note, the hypoxic preconditioning induced an intensified release of EVs enriched with miRNAs involved in different stages of the healing process. Taking advantage of a cardiotoxin (CTX)-induced skeletal muscle injury model, we confirmed a potent EV-mediated anti-inflammatory effect, through the significant downregulation of the inflammatory cytokine *IL6* accompanied by the concomitant upregulation of *IL10*. At the same time we observed also a downregulation of the M1 marker *Nos2* and an increased expression of the putative M2 markers *Arg1* and Ym1, together with an increased percentage of $CD206^{pos}$ cells infiltrating damaged and EV-treated muscles.

Materials and Methods

Mice

C57Bl/6 (MHC H2b haplotype) male mice between 3 and 5 month old were used. All mice were bred and maintained at the Animal Facility of "IRCCS Azienda Ospedaliera Universitaria San Martino – IST, Istituto Nazionale per la Ricerca sul Cancro." All animal procedures were approved by the Local Ethical Committee and performed in accordance with the national current regulations regarding the protection of animals used for scientific purpose (D. Lgs. 4 Marzo 2014, n. 26, legislative transposition of Directive 2010/63/EU of the European Parliament and of the Council of 22 September 2010 on the protection of animals used for scientific purposes).

Adipose Tissue-Derived MSCs Isolation and Culture

Subcutaneous adipose tissue in the form of liposuction aspirates was obtained from human healthy donors ($n = 18$) during routine lipoaspiration after informed consent. Protocol and procedures were approved by the local ethical committee. For more details regarding MSC isolation and characterization, see Supporting Information Materials and Methods.

Bone Marrow-Derived Macrophage Isolation and Culture

Bone marrow (BM)-derived macrophages (Mϕ) were isolated from C57Bl/6 mice by flushing the BM with 5 ml of Phosphate Buffered Saline (PBS), as previously described [10]. Each primary culture was obtained from the BM of 3 mice, and a total of 6 primary cultures were used. Details are in Supporting Information Materials and Methods.

Preparation of MSC Conditioned Media and EV Isolation

EVs were isolated from the conditioned media derived from human MSCs. When cells reached a confluence of 80%, extensive washes in PBS were performed to remove any possible residue of FBS. The cells were transferred in EV-isolation medium (serum-free Dulbecco-Modified Eagle Medium (D-MEM) not supplemented with Fibroblast Growth Factor-2) and the culture split into two subcultures maintained for 48 hours under normoxic (20% O_2) and hypoxic (1% O_2) condition, respectively. EVs were isolated from normoxic- and hypoxic-conditioned media (EV^{Normo} and EV^{Hypo}) by differential centrifugation at 300*g* for 10 minutes, 2,000*g* for 20 minutes, 10,000*g* for 30 minutes at 4°C to eliminate cells and debris. Obtained supernatants were depleted of residual floating cells and cell debris by filtration with 0.22 μm filter units (Merck Millipore Ltd, Vimodrone, MI, Italy), followed by two consecutive steps of ultracentrifugation at 100,000*g* for 90 minutes, including a washing step in PBS, to precipitate EVs. A Beckman Coulter ultracentrifuge (Beckman Coulter Optima L-90K ultracentrifuge; Beckman Coulter, Fullerton, CA) was used with swinging bucket rotors type SW28 and SW41Ti. EVs were collected in 100 μl of filtered PBS and used immediately after isolation.

Transmission Electron Microscopy

The morphological evaluations of isolated EV^{Normo} and EV^{Hypo}, and corresponding MSC monolayers were performed by transmission electron microscopy (TEM). For details, see Supporting Information Materials and Methods.

Protein Quantification and Immunoblot Analysis

Protein contents of isolated EVs were measured using a BCA protein assay kit (Thermo Scientific Pierce, Rockford, IL) following manufacturer's instructions. Sample preparation for immunoblot analysis is described in Supporting Information Materials and Methods.

Stem Cells Translational Medicine published by Wiley Periodicals, Inc. on behalf of AlphaMed Press

Cell Viability and BrdU Cell Proliferation Assay

3×10^4 Mϕ in serum free medium were plated in 96-well plates for 24 hours in the presence or absence of either EV^{Normo} or EV^{Hypo}. Cell proliferation was measured with the use of the Cell Proliferation Enzyme-linked immunosorbent assay (ELISA), Bromodeoxyuridine (BrdU) (Roche Mannheim, Germany), according to the manufacturer's instructions. Five independent experiments were performed.

In vivo Angiogenic Assay

The in vivo angiogenic assay is described in Supporting Information Materials and Methods.

Flow cytometry Analysis

At least nine independent preparations of both EV^{Normo} and EV^{Hypo} were stained with 10 μM Cell Trace (Molecular probes) in combination with the mouse anti-human monoclonal antibody (mAb) CD63 (Clone: H5C6) (BD Pharmingen) or the anti-human mAb CD105 (Clone: SN6) (eBioscience). A set of microsphere suspensions (1, 4 μm) (Molecular Probes) was used as size reference. An unstained sample was acquired to detect the sample autofluorescence and set the photomultiplier for all the three used channels; fluorescent spill-over was controlled by spectral overlap adjustment, acquiring single-color stained tubes. Forward and side scatter channels (FSC and SSC) were used on a logarithmic scale visualized in bi-exponential mode. The FSC and SSC photomultipliers were set using background noise as the lower optical limit, acquiring a sample of sterile PBS tube. The threshold, set on the FSC channel, was regulated to reduce the noise progressively, allocating dots in low left corner of plot, in order to clearly detect EVs. Details about the absolute count of EVs, the immunophenotype of Mϕ cultured in presence/absence of EVs and the immunophenotype of Mϕ infiltrating the injured *tibialis anterior* (TA) muscles are reported in Supporting Information Materials and Methods.

RNA Extraction

RNA extraction procedure for both EV pellet and TA muscles is described in Supporting Information Materials and Methods.

microRNA Profiling

The miRNA fraction of each sample was subjected to stem-loop RT-qPCR amplification, as described in Supporting Information Materials and Methods.

Quantitative Real-Time PCR

To validate the RNA sequencing data, we performed a qPCR analysis of miR-199a-3p, miR-126, miR-223, and miR-146b. Each microRNA was tested on three independent preparations of both EV^{Normo} and EV^{Hypo}, and three independent experiments were performed. The miRNA-specific miScript Primer Assays were purchased from QIAGEN (MS00007602 for miR-199a-3p, MS00003430 for miR-126, MS00003871 for miR-223, and MS00003542 for miR-146b). Details reported in Supporting Information Materials and Methods.

Details about the quantification of *IL-6, IL-10, Nos2, Arg1, Ym1, MCP1, eMyhc, Pax7,* and *MyoD* mRNAs in TA muscles of CTX and EVs injected mice are described in Supporting Information Materials and Methods.

Labeling and Internalization of EVs

EV^{Normo} and EV^{Hypo} (derived from three different MSC cultures) were labeled using PKH67 membrane-binding fluorescent labels according to manufacturer's recommendations (Sigma-Aldrich, Allentown, PA).

Three independent primary cultures of Mϕ seeded on glass slides placed in 24-well plates were incubated at 37°C with labeled EVs at a concentration of 1 μg EVs/10,000 cells. Uptake was stopped after 3 hours by washing and fixation in 4% paraformaldehyde for 20 minutes.

Immunofluorescence Analysis

Immunofluorescence analysis performed on Mϕ is included in Supporting Information Materials and Methods.

Mouse Model of Cardiotoxin-Induced Muscle Injury

Eight-week-old male C57BL/6 mice (six per group) were anesthetized with isoflurane. Twenty microliter of 10 mM cardiotoxin (CTX) (Sigma) in PBS were intramuscularly administered into the TA muscle of both legs. One microgram of EVs (diluted in 20 μl PBS) derived from normoxic and hypoxic MSCs were injected into the right and left TA muscles, respectively. Control mice were treated with 20 μl of vehicle solution. EVs or vehicle solution were injected 2 hours postadministration of CTX and a boost of EVs was done 4 days after muscle injury. Mice were sacrificed after 1, 2, and 7 days post lesion induction and the harvested TA muscles were snap-frozen in liquid nitrogen before further RNA extraction processing.

Histology and Morphometric Analysis

The histological analysis of differentially-treated muscle tissues is described in Supporting Information Materials and Methods.

Statistical Analysis

All results were expressed as mean ± SD or as mean ± SEM from at least three independent experiments. Statistical comparisons between two groups were performed using an unpaired two-tailed Student's *t* test. Differences among multiple groups were statistically analyzed employing One-way ANOVA and Tukey's multiple comparisons test. A p value below.05 was considered to be statistically significant. All statistical analyses were performed using GraphPad Prism Version 6.0a (GraphPad Software, La Jolla, CA).

RESULTS

Hypoxic Conditioning of MSCs Enhances the Release of EVs Endowed With Angiogenic Potential

The cargo and function of EVs depend on their cells of origin, suggesting that intercellular communication through vesicles is a dynamic system, adapting its message depending on the conditions of the producing cells [18]. Changes in oxygen concentrations affect many of the distinctive characteristics of stem and progenitor cells [19]. On this basis, we evaluated whether hypoxic conditioning of human adipose tissue-derived MSCs could influence their EV secretion. Confluent primary MSC cultures fulfilling the minimal criteria proposed by the International Society for Cellular Therapy [20] (Supporting Information Fig. 1A) were maintained for 48 hours in serum-free medium in a normoxic or hypoxic environment. After the starvation period, more than 85%

of MSCs resulted viable in both culture conditions (Supporting Information Fig. 1B). As expected, MSCs cultured in hypoxic conditions had a higher level of HIF-1α expression than those cultured in normoxic conditions (Supporting Information Fig. 1B). After 48 hours of medium conditioning, isolated EV^{Normo} and EV^{Hypo}, and corresponding MSC monolayers (MSC^{Normo} and MSC^{Hypo}) were analyzed by TEM. TEM revealed the presence of larger shedding vesicles (microvesicles) as well as several multivesicular bodies (MVBs) containing exosomes within the cell cytoplasm in both culture conditions, indicating the release of a mixed population of EVs (Fig. 1A). In both samples, EVs appeared with a round-shape morphology, mainly isolated or less frequently aggregated in small groups. They showed a diameter ranging from 40 to 250 nm suggesting that the separation procedure selected a population of nano-scaled vesicles referable mostly but not only to exosomes. No morphological differences between EV^{Normo} and EV^{Hypo} were observed with regard to their size, shape, or electrondensity (Fig. 1A). In order to characterize isolated EVs, immunoblot and flow cytometry analysis were performed. Western blot analysis revealed that both EV^{Normo} and EV^{Hypo} express the specific vesicular protein CD81, member of the tetraspanin family, and Alix, that is involved in MVB formation (Fig. 1B). EV^{Normo} and EV^{Hypo} were further characterized taking advantage of a multiparametric flow cytometry approach. To separate true events from background noise, EVs were defined as events that were included in the dimensional gate of 1 μm, which was established according to a well-defined light scatter profile of beads with absolute size (Fig. 1C). EVs were targeted with the Cell Trace labeling, in order to consider only intact membrane structures, along with either the mesenchymal marker CD105 or the vesicular marker CD63. Both types of Cell Trace labeled-EVs expressed the CD105 and CD63 antigens, but the percentage of EVs co-expressing CD63 was significantly higher in the hypoxic condition compared to the normoxic one ($p < .01$) (Fig. 1D). The absolute quantification of EV^{Normo} and EV^{Hypo} was determined by comparing their events to a known number of fluorescent bead events (Trucount beads, Fig. 1C). The hypoxic conditioning induced a significantly increased release of EVs when compared to the normoxic condition ($p = .0318$) (Fig. 1E).

The observations that the regenerative properties mediated by MSCs, including the ability to stimulate angiogenesis, are mediated by EV secretion, and that hypoxia is a factor that favors the accumulation of pro-angiogenic molecules [21], led us to explore the angiogenic potency of MSC-EVs in vivo by performing the Matrigel plug assay. After 3 weeks of implantation, we observed that EV^{Normo} and EV^{Hypo} induced the formation of vessel-like endothelial structures (Fig. 1F). Matrigel plugs in presence of both types of vesicles were enriched in angiogenic molecules, such as *Pecam1* and *VegfA* when compared with control empty plugs (Fig. 1G). The presence of vessels along the periphery of the plugs was confirmed in all the experimental conditions by hematoxylin and eosin and CD31 immunostaining (Fig. 1H). Noteworthy, in EV^{Hypo}-treated plugs, a higher expression of *Pecam1* and *VegfA* and an increased density of vessels with a larger diameter were detectable (Fig. 1G, 1H).

EVs Secreted Under Hypoxia Express miRNAs Actively Involved in Different Stages of the Healing Process

miRNAs influence many biological processes and can be taken up as EV cargo also by distant cells [22, 23]. To compare the profile of miRNAs present in both EV^{Normo} and EV^{Hypo}, each sample was tested for the expression of 384 different miRNAs by PCR array. In order to identify differentially expressed miRNAs in EVs released under hypoxic conditions, raw data were normalized using the small U6 RNA as endogenous reference. Setting EV^{Normo} as control sample and EV^{Hypo} as test sample, the fold change was calculated dividing the normalized gene expression profile of the test sample by the corresponding control sample. The hypoxic cell treatment during the EV release induced the significant over-expression of 20 miRNAs and the under-expression of 48 miRNAs (Fig. 2A, 2B). We focused on four specific miRNAs that are implicated in the inflammatory (miR-223 and miR-146b) [24–26], proliferative and differentiative phases (miR-126 and mir-199a) [27, 28] of the healing process (Fig. 2C–2F). The significantly upregulated expression of these miRNAs was confirmed by quantitative Real-Time PCR, thus suggesting that hypoxia-driven pathways are critical for successful tissue repair.

MSC-Derived EVs Promote Macrophage Polarization

In the healing process, macrophages mediate the inflammatory phase by maintaining a pro-inflammatory phenotype in order to inhibit possible infections. However, they switch to a pro-resolving, anti-inflammatory phenotype as soon as the initial "emergency" is over [29, 30].

To evaluate the role exerted by EVs in macrophage polarization, we began characterizing the interactions of EVs with recipient cells. We tested whether BM-derived macrophages (Mϕ) were able to internalize both EV^{Normo} and EV^{Hypo}. Mϕ that were incubated for 3 hours in presence of either EV^{Normo} or EV^{Hypo} previously stained with the fluorescent lipophilic membrane-diffuse dye PKH67, efficiently internalized EVs within their cytoplasm (Fig. 3A). This result was also confirmed by flow cytometry analysis performed after the coculture period on responding cells. More than 70% of EV-treated macrophages resulted positive for the expression of the FITC-fluorescent dye PKH67 used to stain EVs and no FITC-positive signal was detectable in untreated macrophages (Fig. 3B). Cell proliferation of recipient Mϕ maintained for 24 hours in serum free culture conditions was evaluated using a BrdU-uptake assay. Macrophage proliferation was significantly increased following treatment with both EV^{Normo} and EV^{Hypo} compared to untreated cells ($p < .0001$), and this increase was even greater in hypoxic conditions compared to the normoxic ($p = .0011$) (Fig. 3C).

The flow cytometric analysis of Mϕ maintained in standard culture medium (Mϕ w/o EVs) or in the presence of either EV^{Normo} or EV^{Hypo} was performed. In standard conditions, Mϕ expressed statistically significant higher levels of the pro-inflammatory M1-like markers Ly6C, CD11b, CD40, and CD86 compared to the EV-treated cells (Ly6C: $p = .0186$; CD11b: $p = .0017$; CD40: $p = .0073$; CD86: $p = .0019$) and did not express any of the typical M2 markers, such as the scavenger receptor CD36, the mannose receptor CD206 or the $\alpha_v\beta_3$ integrin CD51 (Fig. 3D, 3E). Interestingly, 72 hours of treatment with both EV^{Normo} and EV^{Hypo} induced a significant switch of recipient macrophages toward an anti-inflammatory phenotype (CD206: $p < .0001$; CD51: $p = .0126$; CD36: $p = .0027$) (Fig. 3D, 3E). It is noteworthy that EVs that were released under hypoxic conditions exerted a strengthened anti-inflammatory effect compared to EVs released under normoxia, downregulating the expression of the co-stimulatory molecule CD86 and the activation marker CD11b ($p = .0095$ and $p = .0448$, respectively) (Fig. 3E). Taken together, these data indicate that MSC-derived EVs, and in particular those released under hypoxic conditions, actively interact with key

STEM CELLS TRANSLATIONAL MEDICINE published by Wiley Periodicals, Inc. on behalf of AlphaMed Press

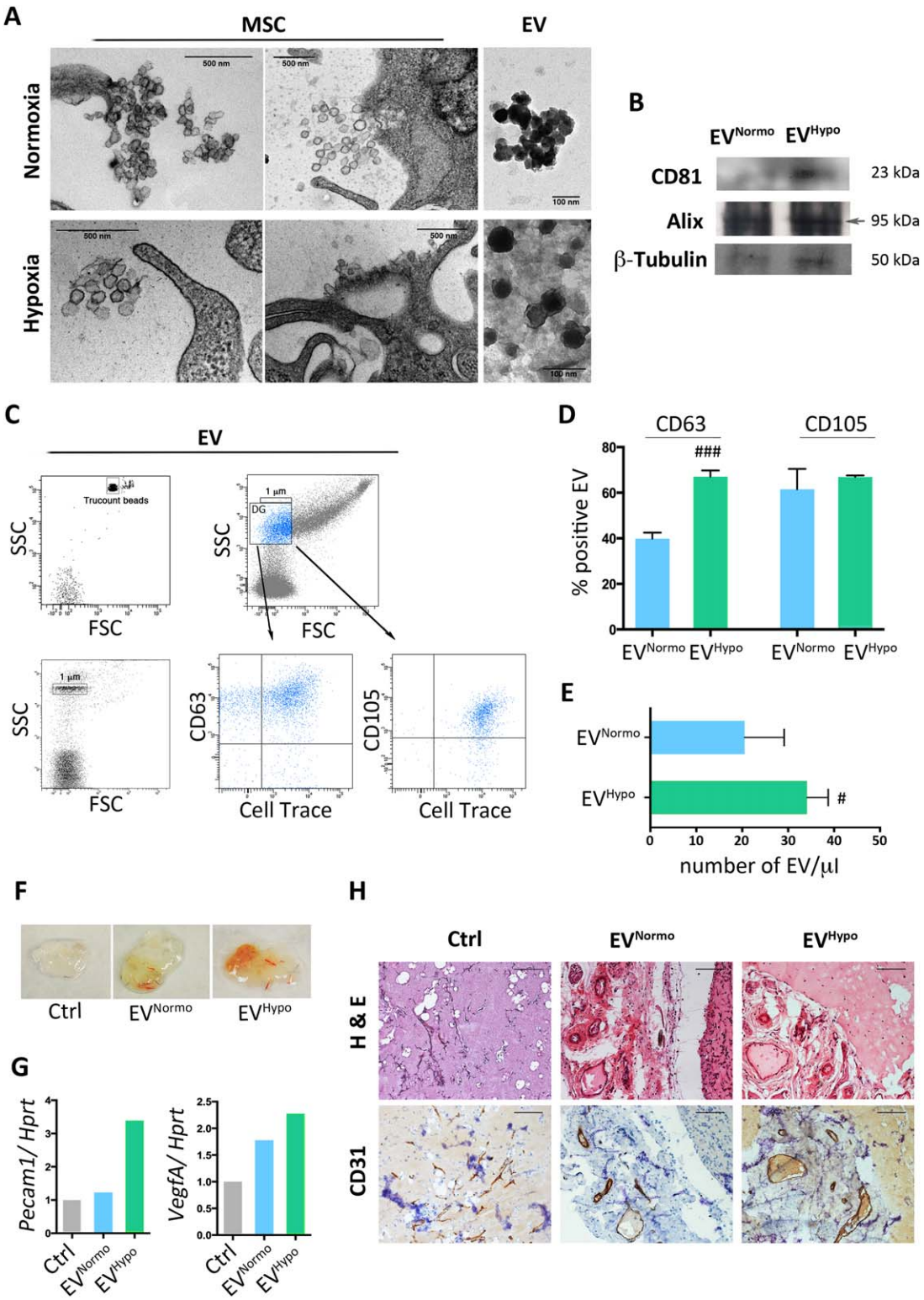

Figure 1. MSC-derived EV characterization. **(A)**: Transmission electron microscopy analysis of MSC cultured for 48 hours in normoxic and hypoxic conditions and corresponding isolated EV^{Normo} and EV^{Hypo}. Scale bars: MSC panels = 500 nm; EV panels = 100 nm. **(B)**: Representative Western blot analysis for EV specific markers (CD81 and Alix) and for β-Tubulin. **(C)**: Flow cytometry strategy adopted to characterize EV^{Normo} and EV^{Hypo}. Vesicles were stained by the lipophilic dye Cell Trace, the vesicular marker CD63 and the MSC marker CD105. **(D)**: Histogram showing the percentage of Cell $Trace^{pos}$ EVs coexpressing CD63 or CD105. Data are presented as mean ± SD. ###, $p = .0003$ (unpaired Student's *t* test). **(E)**: Histogram showing the absolute number of Cell $Trace^{pos}$ EVs quantified trough Trucount fluorescent beads. Data are presented as mean ± SD. #, $p = .0318$ (unpaired Student's *t* test). **(F)**: Representative photo of Matrigel plugs in combination with PBS (Ctrl), 5 µg of EV^{Normo} or 5 µg of EV^{Hypo}, recovered 3 weeks after their in vivo injection. **(G)**: Histograms summarizing densitometric analysis of PCR products normalized to the housekeeping gene *Hprt*. Pecam1; VegfA. **(H)**: Representative histology of Matrigel plug sections stained for hematoxylin and eosin (upper panels) and for the endothelial cell marker CD31 (lower panels). Magnification ×40. Scale bar = 100 µm. Abbreviations: EVs, extracellular vesicles; FSC, forward scatter channels; *Hprt,* hypoxanthine guanine phosphoribosyltransferase; MSCs, mesenchymal stem cells; Pecam1, platelet and endothelial cell adhesion molecule 1; SSC, side scatter channels; VegfA, vascular endothelial growth factor A.

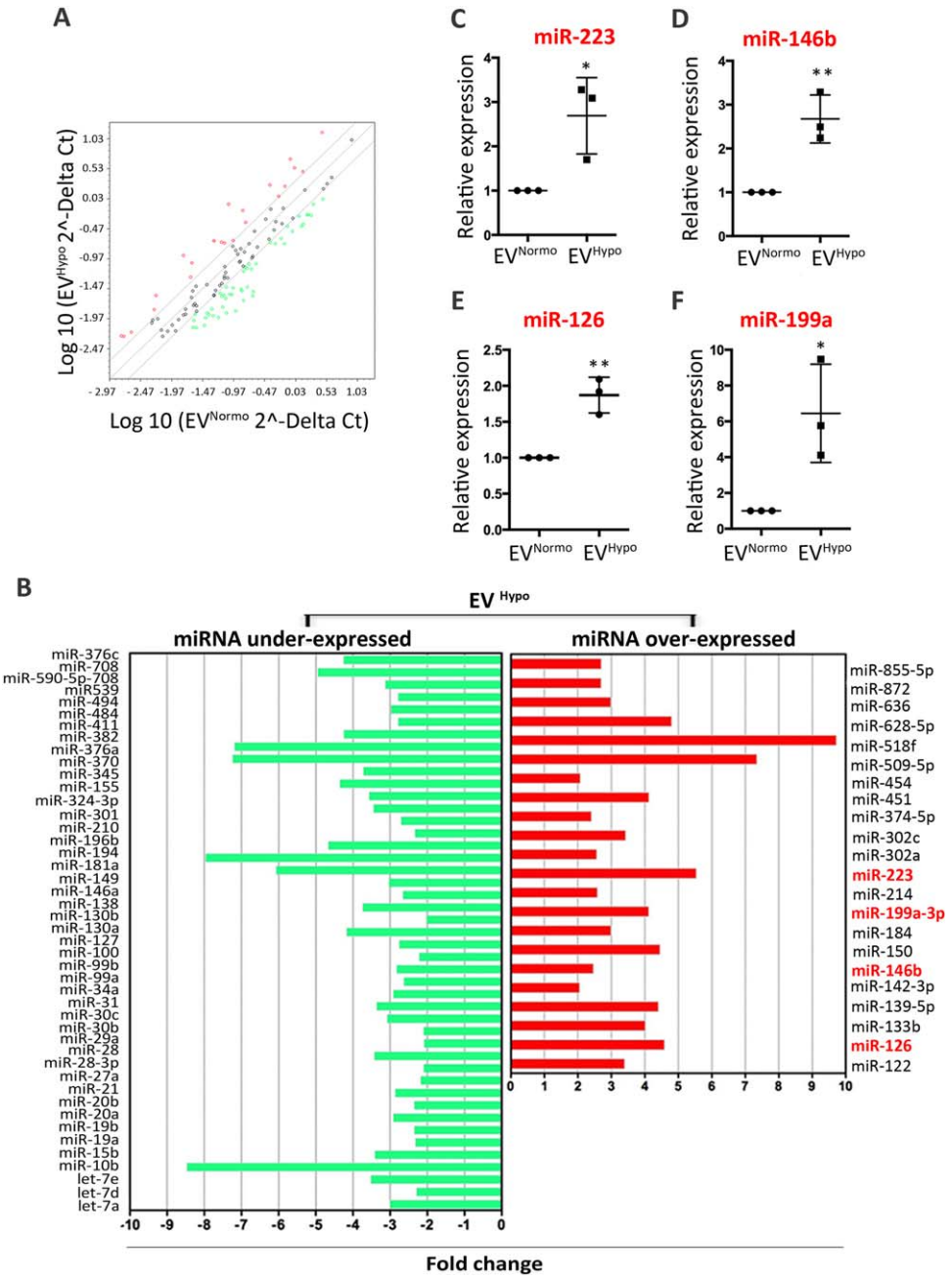

Figure 2. Analysis of miRNAs enriched in EV^{Hypo}. **(A)**: Scatter plot of the human miRNome miScript miRNA PCR Array profile depicting the distribution of differentially expressed miRNAs in EV^{Hypo} versus EV^{Normo}. The graph was obtained by plotting the normalized log10 miRNA expression ($2^{-\Delta Ct}$) in EV^{Hypo} (*y*-axis) divided by the one in the control EV^{Normo} (*x*-axis). Red and green dots represent upregulated and downregulated miRNAs with an expression level >2 or <0.5, respectively. **(B)**: Histografic representation of under-expressed (green) and over-expressed (red) miRNAs isolated in EV^{Hypo}. **(C–F)**: Validation of selected miRNAs expressed by EV^{Normo} and EV^{Hypo} through quantitative real-time PCR. Normalized data were averaged from three independent experiments, and expressed as mean ± SD. **(C)**: miR-223, *, $p = .0274$; **(D)**: miR146b, **, $p = .0062$; **(E)**: miR-126, **, $p = .0038$; (F) miR-199a, *, $p = .0264$ (unpaired Student's *t* test). Abbreviation: EVs, extracellular vesicles.

components of the innate immune system and influence their immunoregulatory and regenerative behavior.

EVs Regulate the M1/M2 Balance of Infiltrating Macrophages in a Skeletal Muscle Injury Model In Vivo

Skeletal muscle has a remarkable capacity for regeneration through a complex injury/repair process that includes inflammation, myofiber regeneration, and angiogenesis [31, 32]. Observations that different Mϕ subsets are associated with different stages of muscle regeneration led us to investigate whether EV treatment could influence macrophage polarization from M1 to M2 phenotype in vivo. We opted for a CTX injury in the mouse TA muscle, a reproducible model that recapitulates all healing phases. Muscles, subjected to CTX-damage followed by injection

Stem Cells Translational Medicine published by Wiley Periodicals, Inc. on behalf of AlphaMed Press

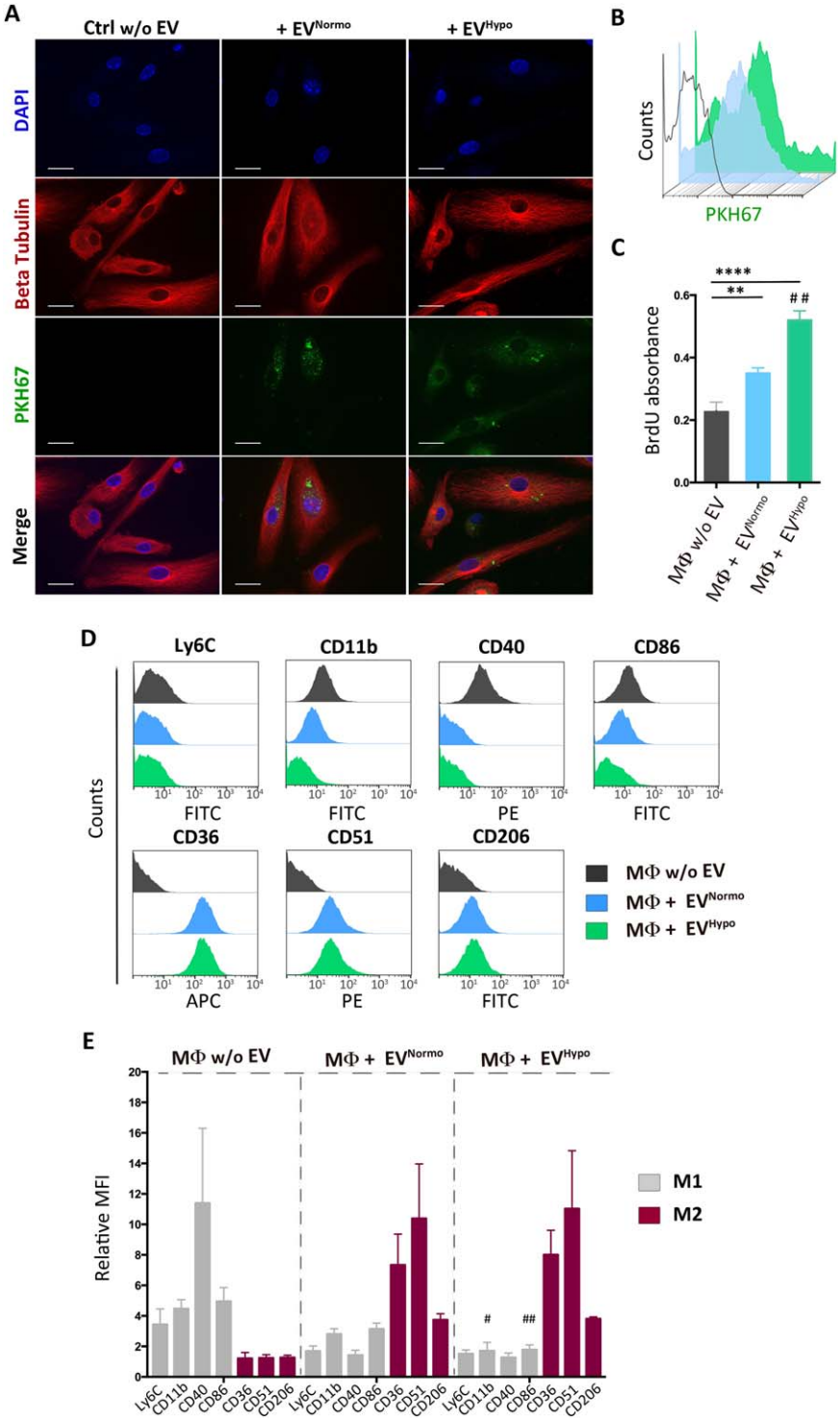

Figure 3. MSC-derived EVs trigger macrophage (Mϕ) proliferation and polarization. **(A)**: Immunofluorescence analysis of MΦ cocultured for 3 hours in a serum-free (SF) medium without EVs (Ctrl w/o EV), and with either normoxic or hypoxic PKH67-labeled EVs (EV^{Normo} and EV^{Hypo}). DAPI (blue), β-tubulin (red), PKH67 (green). Magnification ×63. Scale bar =20 μm. **(B)**: Flow cytometry analysis of MΦ cocultured for 3 hours without EVs (gray line) and with normoxic (light blue line) and hypoxic (green line) PHK67-labeled EVs. **(C)**: Proliferation inductive effect of EV^{Normo} and EV^{Hypo} on MΦ following 24 hour incubation with 10 μM BrdU, compared to the control (MΦ w/o EV). The average of three independent experiments is shown. Statistical significance was determined using ANOVA (**, $p = .0031$; ****, $p < .0001$) and unpaired Student's *t* test to compare EV^{Normo} versus EV^{Hypo} (##, $p = .0011$). (**D**) Representative dot plots of phenotypic characterization of MΦ cultured for 72 hours in SF standard medium (MΦ w/o EV, gray line), and in SF medium containing 1 μg of EV^{Normo} ($MΦ + EV^{Normo}$, light blue line) and EV^{Hypo} ($MΦ + EV^{Hypo}$, green line). Ly6C , CD11b, CD40, and CD86 were selected as markers of pro-inflammatory MΦ (M1); CD36, CD51, CD206 as markers of anti-inflammatory MΦ (M2). **(E)**: Histogram presenting the data already shown in panel **(D)** as relative mean fluorescent intensity. In gray are indicated selected M1 markers and in purple M2 markers. Each column is the average of three independent experiments. Statistical significance was determined using an unpaired Student's *t* test. #, $p = .0448$; ##, $p = .0095$. Abbreviations: DAPI, 4',6-diamidino-2-phenylindole; FITC, Fluorescein isothiocyanate; EVs, extracellular vesicles.

of either EV^{Normo} or EV^{Hypo}, were examined at different times (Fig. 4A). One day after CTX injection, the histopathological evaluation of muscle damage was performed in all experimental groups. Normal myofibers with uniform size, poligonal shape and peripheral nuclei were observed in untreated mice (naive) (Fig. 4B). Following injury, CTX-treated mice, as well as EV^{Normo} and EV^{Hypo} treated animals, had extensive necrotic muscle fibers with vigorous mononuclear cell infiltrate (Fig. 4B). However, at day 1 and 2 post-lesion induction, the ratio between *IL6* and *IL10* cytokines (*IL6/IL10*) progressively decreased in EV-treated muscles compared to CTX-treated controls (day1: $p = .0024$; day 2: $p < .0001$), thus indicating that the injection of both types of EVs significantly mitigated the inflammatory milieu within the injured tissues (Fig. 4C). At day 2, this observation was accompanied by a significant increase in both types of EV-treated muscles of the M2 markers Arginase 1 (*Arg1*) and Chitinase 3-like 3 (*Ym1*) ($p = .0453$ and $p = .0087$, respectively), parallel to a decreased expression of the M1 marker Nitric Oxide Synthase 2 (*Nos2*) (Fig. 4D–4F). The latter results were also confirmed by flow cytometry, analyzing the cells recovered from the damaged and/or EV-treated muscles. The percentage of CD206-positive ($CD206^{pos}$) Mϕ compared to the percentage of Ly6C-positive ($Ly6C^{pos}$) cells was significantly higher within the cells recovered from EV^{Hypo}-treated muscles compared to both CTX-treated and EV^{Normo}-treated samples ($p = .0006$) (Fig. 4G). Given the important role of Mϕ in muscle regenerative activities, chemokines that are known to attract and interact with these innate immune cells play pivotal roles in the process of muscle recovery after an injury. Among the others, monocyte chemoattractant protein-1 (MCP-1) coordinates inflammation-dependent events involved in muscle regeneration [33]. Interestingly, at day 2 post-lesion induction, the expression level of *MCP-1* was significantly upregulated in EV^{Hypo}-treated muscles compared to other experimental conditions ($p = .028$) (Supporting Information Fig. 2A). Since CTX-induced skeletal muscle injury is an optimal model of muscle self-repair, we analyzed key genes playing a dominant role during the overlapping regeneration and remodeling phases that follow inflammation. At day 7, when compared to CTX-treated and EV^{Normo}-treated muscles, EV^{Hypo}-treated muscles presented a significant upregulation of both Paired Domain Transcription Factor 7 (*Pax7*) and Myogenic Differentiation Antigen (*MyoD*) genes, selectively expressed by activated satellite cells ($p = .048$ and $p = .0006$, respectively), as well as of embryonic myosin heavy chain (*eMyhc*), expressed by regenerating fibers ($p = .018$) (Supporting Information Fig. 2B). Concurrently, the progression of muscle regeneration and the prospective differences between EV-treated and CTX-treated muscles were confirmed by histological observations. As expected, many newly formed centrally nucleated fibers were present in CTX-treated muscles (Supporting Information Fig. 2C). It's well known that multinucleated muscle fibers form from the fusion of mononucleated myoblasts [34]. We observed that the number of mononucleated myoblasts was significantly decreased in both types of EV-treated muscles, compared to the CTX controls (Supporting Information Fig. 2C–2E, 2G). Interestingly, in the same EV-treated muscles the number of fibers containing two or more centrally located nuclei was significantly increased compared to the CTX-injured muscles, and this increase was greater followed EV^{Hypo} injection (Supporting Information Fig. 2C, 2D, 2F, 2G). These results suggest that MSC-derived EVs, and in particular those released under hypoxic conditions, accelerate the muscle regeneration process.

Discussion

EVs represent novel players in various cell communication systems, being involved in the regulation of many routes of signaling pathways and intercellular information transfer [35]. It is thanks to their vast amount of properties that EVs have been successfully applied in different fields, such as tumor biology, immunology and regenerative medicine [36].

Stem/progenitor cells and in particular MSCs are active biological components of many regenerative medicine therapies [37]. Recent efforts in elucidating mechanisms of action of these therapies have revealed an increasingly important role of the cell paracrine activity in enhancing positive outcomes without a significant cell engraftment [13, 38]. We recently demonstrated a new role of MSCs in wound healing, showing that they can act as modulators of the inflammatory response, secreting cytokines and factors able to induce the switch of pro-inflammatory macrophages toward a pro-resolving, anti-inflammatory phenotype [10]. Indeed, the initial inflammation underlying all regenerative processes is finely coordinated to obtain an efficient outcome, and an altered identity of the inflammatory infiltrate can result in a persistent rather than resolved inflammatory phase [39]. Macrophages, that are an essential component of the inflammatory infiltrate, play important roles in the maintenance of tissue homeostasis [40]. In response to different signals, macrophages are subjected to a reprogramming and undergo two different polarization states that mirror the Th1/Th2 nomenclature [41]. Classical activated M1 macrophages, induced by interferon-γ alone or in combination with microbial stimuli and/or inflammatory cytokines, exert pro-inflammatory activities. On the contrary, cytokines such as IL-4 and IL-13 induce an alternative activation of M2 macrophages, which become involved in inflammation resolution [42].

Since secreted vesicles represent a relevant component of the MSC regenerative milieu [43], in the present study we investigated the possible role of EVs in modulating the MSC paracrine capacity to actively interact with innate immune cells. Given that the presence of areas of hypoxia is a prominent feature of various inflamed, diseased tissues contributing to modulate the MSC regenerative milieu, these interactions were evaluated after both normoxic and hypoxic cell conditioning [44]. We showed that: (a) hypoxic conditioning induced an increased secretion of EVs by MSCs, enriching the EV content in microRNAs involved in different phases of the healing process; (b) MSC-EVs acted as "switchers" of macrophage polarization toward an anti-inflammatory phenotype. The latter result was observed both in vitro and in vivo in a mouse model of skeletal muscle regeneration. Literature reports indicate that hypoxia conditioning of MSCs regulates the cargo and protein packaging into EVs [45]. As herein shown, the higher expression of both pro-angiogenic factors and specific microRNAs, such as miR-223, miR-146b, miR126, and miR-199a in response to hypoxia could be at least in part due to a higher number of EVs released by MSCs. Among microRNAs carried by EVs, miR-223 represents a novel regulator of macrophage polarization, being responsible of suppressing classic pro-inflammatory pathways and enhancing the alternative anti-inflammatory responses, whereas the enforced expression of mir-146b in human monocytes leads to a significant reduction in the production of several pro-inflammatory cytokines and chemokines, such as IL6 [25]. In addition, the increased expression pattern of miR-126 and miR-199a plays important roles in the repair process restoring vascular integrity and inducing cell differentiation, respectively [27, 28].

Stem Cells Translational Medicine published by Wiley Periodicals, Inc. on behalf of AlphaMed Press

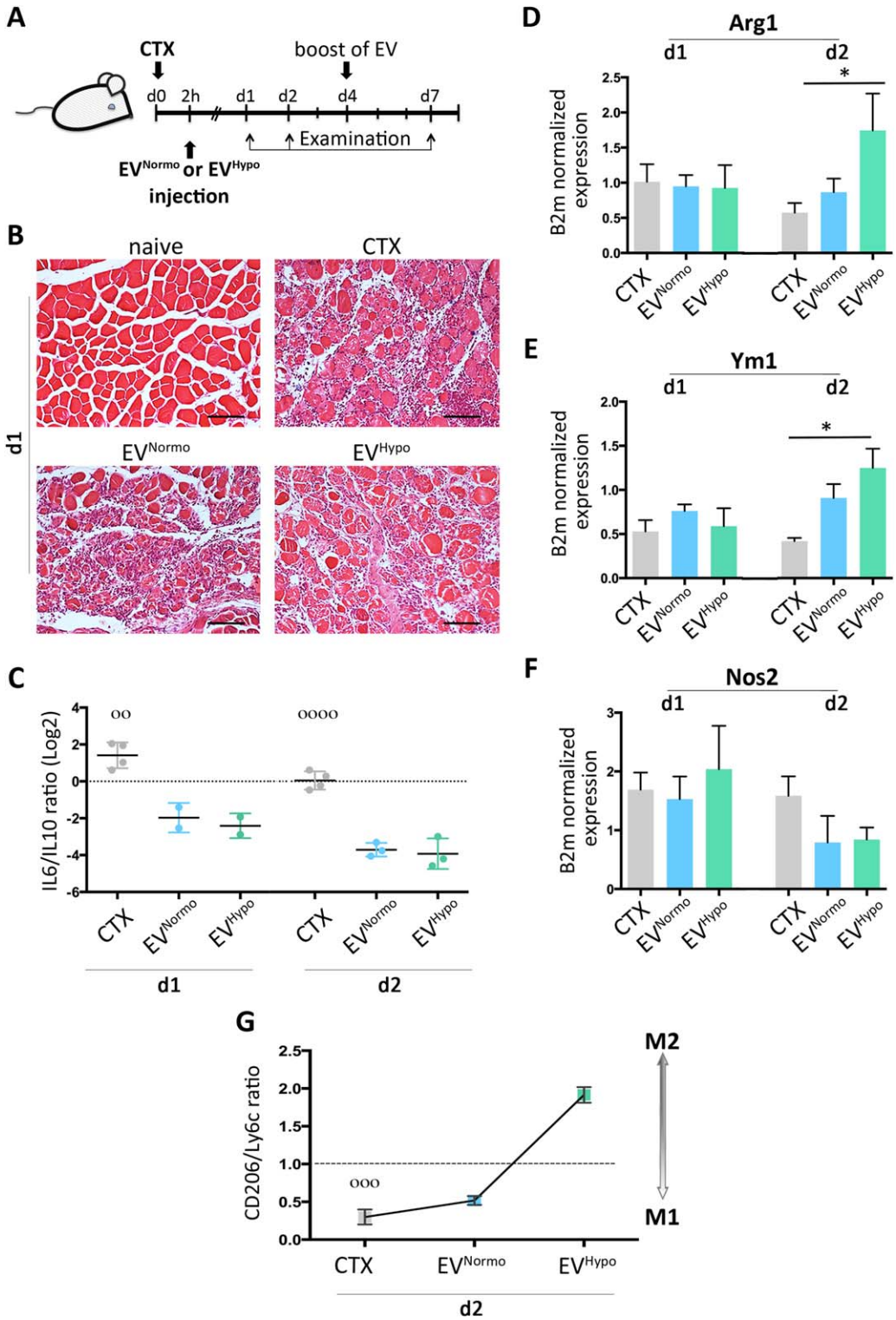

Figure 4. MSC-derived EVs play direct effects on M1/M2 balance in a mouse model of cardiotoxin-induced injury. **(A)**: Schematic diagram of the experimental plan, illustrating the timelines of *tibialis anterior* (TA) muscle examination after CTX-injury and EV-injection. **(B)**: Representative hematoxylin and eosin (H&E) staining of TA muscles derived from naive C57Bl/6 mouse, CTX-treated mouse (upper left and upper right panels, respectively), and from EV^{Normo}- and EV^{Hypo}-treated mice (bottom left and bottom right panels, respectively), one day after damage induction. Magnification ×20. Scale bar = 100 μm. **(C)**: Quantitative real-time PCR analysis of pro-inflammatory (IL6) and anti-inflammatory (IL10) cytokynes in TA muscles derived from mice treated with CTX (gray) alone or in combination with 1 μg EV^{Normo} (light blue) or EV^{Hypo} (green), at 1 and 2 days post-damage induction. Data are presented as log2 of mean expression ratio ± SEM. Statistical significance was determined using ANOVA. ^{oo}, $p = .0024$; ^{oooo}, $p < .0001$. **(D–F)**: Quantitative RT-PCR for selected M1 (Nos2) and M2 (Arg1, Ym1) markers in CTX (gray), EV^{Normo} (light blue) and EV^{Hypo} (green), at 1 and 2 days post-CTX injury. B2m has been used as a housekeeping gene. Data are shown as mean ± SEM. Statistical significance was determined using ANOVA and Tukey's multiple comparisons test; (D) *, $p = .0453$. (E) *, $p = .0087$. **(G)**: Flow cytometry analysis of MΦ subtypes recovered in the treated TA muscles (CTX, EV^{Normo} and EV^{Hypo}) after 2 days. Data are presented as mean expression ratio between CD206 (M2) and Ly6C (M1). ^{ooo}, $p = .0006$ (ANOVA). Abbreviations: Arg1, Arginase 1; CTX, cardiotoxin; EVs, extracellular vesicles; Nos2, nitric oxide synthase 2.

An increasing number of literature reports indicate that MSCs possess the capacity to reduce inflammation and to promote tissue repair processes by their paracrine activity [13, 46]. In particular, it was recently reported that lipopolysaccharide preconditioning of umbilical cord-MSCs increased the secretion of exosomes, responsible for the switch of macrophages to a M2-like profile [47]. In line with this evidence, we here demonstrated for the first time that adipose tissue derived-MSCs release EVs endowed with potent anti-inflammatory capacities to balance macrophage polarization toward a M2 profile, especially after hypoxic pre-treatment. The in vitro stimulation of GM-CSF treated macrophages with either EV^{Normo} or EV^{Hypo} led responding cells to increase their proliferation rate and progressively acquire a M2 phenotype characterized by the expression of CD206, CD51, and CD36. The proper requirement for macrophages is a key feature for efficient muscle regeneration [31, 32]. Indeed, macrophages exert specific functions all through the inflammatory response following muscle damage, which includes the sequential release of pro-inflammatory effectors, the phenotype shift and the activation of myogenic precursors [33]. In this context, CTX-induced skeletal muscle damage represents a highly reproducible model useful to study each step of the inflammatory cascade. The expression level of the typical pro-inflammatory, Th-1 cytokine *IL6* was significantly downregulated in EV-treated muscles at day 1 and 2 post-lesion induction, that represents the timeframe in which maximum macrophage infiltration occurs [48]. This was strictly associated with a significant upregulation of *IL10*, a cytokine that contributes to promote an anti-inflammatory microenvironment [49]. At the same times, the dynamics of macrophage activation marker expression in response to EV administration were investigated. At day 2 the early marker of innate and classical activation *Nos2* was downregulated whereas the expression of *Arg1* and *Ym1*, late markers of alternative activation, were upregulated. This effect was even greater following EV^{Hypo} administration. In the EV-treated muscles, the changes in the expression of these early/late markers coincided with an increased percentage of $CD206^{pos}$ macrophages. MCP-1, also known as CCL2, is important in macrophage recruitment and activation. Mice deficient in CCL2/MCP1 show impaired muscle regeneration, characterized by a decrease in the diameter of the new myofibers, a reduced number of capillaries, and fat accumulation [50]. In our experimental setting, the administration of hypoxic vesicles determined, at day 2, an accumulation of *MCP-1* parallel to the macrophage shift toward a M2 phenotype. These concomitant events could underlie the increased expression, at day 7, of the myogenic markers *Pax7* and *MyoD*, that are upregulated and activated by satellite cells, the increased expression of *eMyhc*, that is upregulated by regenerating myofibers, as well as the significantly increased number of newly formed multinucleated muscle fibers, thus indicating an acceleration of tissue repair triggered by EV administration.

When developing novel regenerative medicine strategies, the rational control of inflammation represents a critical aspect to consider. In this context, the anti-inflammatory, pro-regenerative effects mediated by MSC-EVs could be exploited for therapeutic purposes. From a translational perspective, the use of EVs, in comparison to either traditional cell-based therapies or more recent cell-free strategies based on the use of MSC secretome, presents undeniable advantages. Compared with traditional cell-based therapies, the benefits underlying the use of EVs arise in the possibility to develop safer cell-free therapeutic approaches that could overcome the regulatory obstacles and clinical risks associated to the use of transplanted progenitor cells. Compared to the use of poorly characterized soluble factors, the advantage relies on the ability of EVs to interact and reprogram the surrounding microenvironment, which is a consequence of the variety of their cargo, therefore influencing many biological processes, in particular in injured tissues.

Conclusion

This study demonstrates that MSCs cultured under both normoxic and hypoxic conditions release EVs endowed with anti-inflammatory effects. When co-cultured with responding BM-derived macrophages, EVs are efficiently internalized by responding cells, inducing, in the short term, an increase in their proliferation rate, and shifting the balance toward a M2 pro-resolving phenotype. A significant enrichment in microRNAs involved in different phases of the healing process was detectable in EVs especially in the ones derived from hypoxia conditioned MSCs. Direct administration of EVs in a CTX-induced skeletal muscle injury reduced the inflammatory response, upregulating key markers of alternative activation patterns, and accelerating the expression of myogenic markers. These effects were even greater following EV^{Hypo} administration. Although additional investigations on the mechanisms underlying the therapeutic effects of MSC-EVs is still necessary before proceeding with clinical trials, these results already provide the basis for the use of EVs as an alternative cell-free approach for the induction of regenerative processes.

Acknowledgments

This work was supported in part by POR-FESR funds of Regione Liguria to R.C. and in part by the Italian Ministry of Health ("Young Investigator Grant" - GR-2013-02357519) to R.T.

Author Contributions

C.L.S.: conception and design, collection and/or assembly of data, data analysis and interpretation, manuscript writing; D.R.L.P., C.F., and M.P.: collection and/or assembly of data, data analysis and interpretation; C.B., V.U., E.P., and P.B.: collection and/or assembly of data; M.C.B.: Provision of study material or patients; L.V.: provision of study material or patients, collection and/or assembly of data; R.C.: conception and design, financial support; R.T.: conception and design, financial support, collection and/or assembly of data, data analysis and interpretation, manuscript writing.

Disclosure of Potential Conflicts of Interest

The authors indicate no potential conflicts of interest.

References

1 Goichberg P. Current understanding of the pathways involved in adult stem and progenitor cell migration for tissue homeostasis and repair. Stem Cell Rev 2016; 12:421–437.

2 Gurtner GC, Werner S, Barrandon Y et al. Wound repair and regeneration. Nature 2008; 453:314–321.

3 Velnar T, Bailey T, Smrkolj V. The wound healing process: An overview of the cellular and molecular mechanisms. J Int Med Res 2009;37: 1528–1542.

Stem Cells Translational Medicine published by Wiley Periodicals, Inc. on behalf of AlphaMed Press

4 Eming SA, Krieg T, Davidson JM. Inflammation in wound repair: Molecular and cellular mechanisms. J Invest Dermatol 2007;127: 514–525.

5 Anghelina M, Krishnan P, Moldovan L et al. Monocytes/macrophages cooperate with progenitor cells During neovascularization and tissue repair: Conversion of cell columns into fibrovascular bundles. Am J Pathol 2006;168:529–541.

6 Lolmede K, Campana L, Vezzoli M et al. Inflammatory and alternatively activated human macrophages attract vessel-associated stem cells, relying on separate HMGB1- and MMP-9-dependent pathways. J Leukoc Biol 2009;85:779–787.

7 Das A, Sinha M, Datta S et al. Monocyte and macrophage plasticity in tissue repair and regeneration. Am J Pathol 2015;185:2596–2606.

8 Phinney DG, Prockop DJ. Concise review: Mesenchymal stem/multipotent stromal cells: The state of transdifferentiation and modes of tissue repair--current views. Stem Cells 2007; 25:2896–2902.

9 Dimarino AM, Caplan AI, Bonfield TL. Mesenchymal stem cells in tissue repair. Front Immunol 2013;4:201.

10 Ulivi V, Tasso R, Cancedda R et al. Mesenchymal stem cell paracrine activity is modulated by platelet lysate: Induction of an inflammatory response and secretion of factors maintaining macrophages in a proinflammatory phenotype. Stem Cells Dev 2014;00: 1–12.

11 Bollini S, Gentili C, Tasso R et al. The regenerative role of the fetal and adult stem cell secretome. J Clin Med 2013;2:302–327.

12 Ratajczak MZ, Kucia M, Jadczyk T et al. Pivotal role of paracrine effects in stem cell therapies in regenerative medicine: Can we translate stem cell-secreted paracrine factors and microvesicles into better therapeutic strategies? Leukemia 2012;26:1166–1173.

13 Tasso R, Ulivi V, Reverberi D et al. In vivo implanted bone marrow-derived mesenchymal stem cells trigger a cascade of cellular events leading to the formation of an ectopic bone regenerative niche. Stem Cells Dev 2013; 22:3178–3191.

14 Bang C, Thum T. Exosomes: New players in cell-cell communication. Int J Biochem Cell Biol 2012;44:2060–2064.

15 Camussi G, Deregibus MC, Bruno S et al. Exosomes/microvesicles as a mechanism of cell-to-cell communication. Kidney Int 2010; 78:838–848.

16 Lötvall J, Hill AF, Hochberg F et al. Minimal experimental requirements for definition of extracellular vesicles and their functions: A position statement from the International Society for Extracellular Vesicles. J Extracell Vesicles 2014;3:26913.

17 Ranganath SH, Levy O, Inamdar MS et al. Harnessing the mesenchymal stem cell secretome for the treatment of cardiovascular disease. Cell Stem Cell 2012;10:244–258.

18 De Jong OG, Van Balkom BWM, Schiffelers RM et al. Extracellular vesicles: Potential roles in regenerative medicine. Front Immunol 2014;5:608.

19 Grayson WL, Zhao F, Bunnell B et al. Hypoxia enhances proliferation and tissue formation of human mesenchymal stem cells. Biochem Biophys Res Commun 2007;358:948–953.

20 Martin I, De Boer J, Sensebe L. A relativity concept in mesenchymal stromal cell manufacturing. Cytotherapy 2016;16:613–620.

21 Kholia S, Ranghino A, Garnieri P et al. Extracellular vesicles as new players in angiogenesis. Vasc Pharmacol 2016;S1537–1891: 30105–30101.

22 Valadi H, Ekström K, Bossios A et al. Exosome-mediated transfer of mRNAs and microRNAs is a novel mechanism of genetic exchange between cells. Nat Cell Biol 2007;9: 654–659.

23 Lee Y, El Andaloussi S, Wood MJA. Exosomes and microvesicles: Extracellular vesicles for genetic information transfer and gene therapy. Hum Mol Genet 2012;21:125–134.

24 Zhuang G, Meng C, Guo X et al. A novel regulator of macrophage activation: miR-223 in obesity-associated adipose tissue inflammation. Circulation 2012;125:2892–2903.

25 Curtale G, Mirolo M, Renzi TA et al. Negative regulation of Toll-like receptor 4 signaling by IL-10-dependent microRNA-146b. Proc Natl Acad Sci USA 2013;110: 11499–11504.

26 Sonkoly E, Pivarcsi A. microRNAs in inflammation. Int Rev Immunol 2009;28:535–561.

27 Wang S, Aurora AB, Johnson BA et al. The endothelial-specific microRNA miR-126 governs vascular integrity and angiogenesis. Dev Cell 2008;15:261–271.

28 Jia L, Li Y-F, Wu G-F et al. MiRNA-199a-3p regulates C2C12 myoblast differentiation through IGF-1/AKT/mTOR signal pathway. Int J Mol Sci 2014;15:296–308.

29 Mantovani A, Biswas SK, Galdiero MR et al. Macrophage plasticity and polarization in tissue repair and remodelling. J Pathol 2013;229:176–185.

30 Novak ML, Koh TJ. Macrophage phenotypes during tissue repair. J Leukoc Biol 2013; 93:875–881.

31 Wang H, Melton DW, Porter L et al. Altered macrophage phenotype transition impairs skeletal muscle regeneration. Am J Pathol 2014;184:1167–1184.

32 Chazaud B. Inflammation during skeletal muscle regeneration and tissue remodeling: Application to exercise-induced muscle damage management. Immunol Cell Biol 2016;94:140–145.

33 Shireman PK, Contreras-Shannon V, Reyes-Reyna SM et al. MCP-1 parallels inflammatory and regenerative responses in ischemic muscle. J Surg Res 2006;134:145–157.

34 Folker ES, Baylies MK. Nuclear positioning in muscle development and disease. Front Physiol 2013;4:363.

35 Yáñez-Mó M, Siljander PR-M, Andreu Z et al. Biological properties of extracellular vesicles and their physiological functions. J Extracell vesicles 2015;4:27066.

36 Lener T, Gimona M, Aigner L et al. Applying extracellular vesicles based therapeutics in clinical trials - an ISEV position paper. J Extracell vesicles 2015;4:30087.

37 Chen Y, Shao JZ, Xiang LX et al. Mesenchymal stem cells: A promising candidate in regenerative medicine. Int J Biochem Cell Biol 2008;40:815–820.

38 Tasso R, Gaetani M, Molino E et al. The role of bFGF on the ability of MSC to activate endogenous regenerative mechanisms in an ectopic bone formation model. Biomaterials 2012;33:2086–2096.

39 White ES, Mantovani AR. Inflammation, wound repair, and fibrosis: Reassessing the spectrum of tissue injury and resolution. J Pathol 2013;229:141–144.

40 Wynn TA, Vanella KM. Macrophages in tissue repair, regeneration, and fibrosis. Immunity 2016;44:450–462.

41 Locati M, Mantovani A, Sica A. Macrophage activation and polarization as an adaptive component of innate immunity. Adv Immunol 2013;120:163–184.

42 Martinez FO, Gordon S. The M1 and M2 paradigm of macrophage activation: Time for reassessment. F1000Prime Rep 2014;6:13.

43 Baglio SR, Rooijers K, Koppers-Lalic D et al. Human bone marrow- and adipose-mesenchymal stem cells secrete exosomes enriched in distinctive miRNA and tRNA species. Stem Cell Res 2015;6:127.

44 Murdoch C, Muthana M, Lewis CE. Hypoxia regulates macrophage functions in inflammation. J Immunol 2005;175:6257–6263.

45 Bian S, Zhang L, Duan L et al. Extracellular vesicles derived from human bone marrow mesenchymal stem cells promote angiogenesis in a rat myocardial infarction model. J Mol Med. 2014;92:387–397.

46 Maxson S, Lopez EA, Yoo D et al. Concise review: Role of mesenchymal stem cells in wound repair. Stem Cells Transl Med 2012;1: 142–149.

47 Dongdong T, Haojie H, Chuan T et al. LPS-preconditioned mesenchymal stromal cells modify macrophage polarization for resolution of chronic inflammation via exosome-shuttled let-7b. J Transl Med 2015;13:308–321.

48 Kharraz Y, Guerra J, Mann CJ et al. Macrophage plasticity and the role of inflammation in skeletal muscle repair. Mediators Inflamm 2013;2013:491497.

49 Makita N, Hizukuri Y, Yamashiro K et al. IL-10 enhances the phenotype of M2 macrophages induced by IL-4 and confers the ability to increase eosinophil migration. Int Immunol. 2015;27:131–141.

50 Gondin J, Théret M, Duhamel G et al. Myeloid HIFs are dispensable for resolution of inflammation during skeletal muscle regeneration. J Immunol 2015;194:3389–3399.

See www.StemCellsTM.com for supporting information available online.